electronics

MDPI

Article

Fuel Cell Hybrid Model for Predicting Hydrogen Inflow through Energy Demand

José-Luis Casteleiro-Roca [1,†], Antonio Javier Barragán [2,†], Francisca Segura Manzano [2,†], José Luis Calvo-Rolle [1,*,†] and José Manuel Andújar [2,†]

1 University of A Coruña, Department of Industrial Engineering, Avda. 19 de febrero s/n, 15495 Ferrol, A Coruña, Spain; jose.luis.casteleiro@udc.es

2 University of Huelva, Department of Electronic Engineering, Computer Systems and Automatic, Campus de El Carmen, 21071 Huelva, Spain; antonio.barragan@diesia.uhu.es (A.J.B.); francisca.segura@diesia.uhu.es (F.S.M.); andujar@diesia.uhu.es (J.M.A.)

* Correspondence: jlcalvo@udc.es; Tel.: +34-881-013-117

† These authors contributed equally to this work.

Received: 4 October 2019; Accepted: 7 November 2019; Published: 10 November 2019

Abstract: Hydrogen-based energy storage and generation is an increasingly used technology, especially in renewable systems because they are non-polluting devices. Fuel cells are complex nonlinear systems, so a good model is required to establish efficient control strategies. This paper presents a hybrid model to predict the variation of H2 flow of a hydrogen fuel cell. This model combining clusters' techniques to get multiple Artificial Neural Networks models whose results are merged by Polynomial Regression algorithms to obtain a more accurate estimate. The model proposed in this article use the power generated by the fuel cell, the hydrogen inlet flow, and the desired power variation, to predict the necessary variation of the hydrogen flow that allows the stack to reach the desired working point. The proposed algorithm has been tested on a real proton exchange membrane fuel cell, and the results show a great precision of the model, so that it can be very useful to improve the efficiency of the fuel cell system.

Keywords: fuel cell; hydrogen energy; intelligent systems; hybrid systems; artificial neural networks; power management

1. Introduction

The climate change and the problems derived from the pollution have caused society to look for new source of energy, especially clean energy sources. The hybrid energy topologies, where classical power plants and energy storage are combined, are some of the most promising technologies. The hydrogen is a possible technology to use in storage systems; the hydrogen can be produced with electrolyzers, storage, and then used in fuel cell to produce electrical power [1].

The main challenge of storage systems is the efficiency improvement in general terms. However, from a useful point of view, this efficiency is frequently measured in economic terms. Obviously, before reaching this profitable objective, there is conscientious development. During the last times, there are a lot of different proposals for achieving energy storage systems, in some different ways. For instance, in [2], an optimal nonlinear controller based on model predictive control (MPC) for a flywheel energy storage system is proposed in which the constraints on the system states and actuators are taken into account. The authors in [3] described a system for storing energy deep underwater in concrete spheres which also can act as moorings for floating wind turbines. A proposal is made in [4] for a deterministic and an interval unit commitment formulation for the co-optimization of controllable

generation and PHES (pumped hydro energy storage), including a representation of the hydraulic constraints of the PHES.

The fuel cell systems are still researched, and its performance could increase in a few years. This is a high reliability choice for steady applications like electrical vehicles or space applications and, moreover, it is a clean energy source [5]. Internally, a fuel cell is a combination of small individual cells that are connected to create a stack. In the stack, an electrochemical reaction produces the electrical power when the hydrogen (H_2) is combined with the oxygen (O_2) in a specific environment. A control system ensures that the whole operation is performed in a safe condition, using some subsystems (cooling, conditioning the gases, inlet system, etc.) [6].

In different clean technologies, like photovoltaic or wind generation, the power production depends on the availability of the primary energy (sun or wind). The fuel cells do not depend on other energy than H_2 have, and such a thing allows for installing it wherever it is necessary. A Proton Exchange Membrane Fuel Cell (PEMFC) is one of the most efficient technologies, as it has high energy density, low volume, and weight against other fuel cells. It operates at a low temperature (less than 100 °C), and this allows for using less time to heat when it starts working. It has a large range of power that can adapt to a lot of applications [5]. High power fuel cells could be used connected to the electrical network in power stations [7–11]—while smaller systems could be used in mobile stations [12]. Apart from the output power, the energy stored (the power during the time that can be produced) depends only on the amount of H_2 available.

The output of the fuel cell is considered as a non-regulated power, as it is produced by an electrochemical reaction. It needs a system to control the H_2 and O_2 inlet flow, and also to ensure the security of the whole system. Moreover, the electrical output values can vary by, for example, external agents like temperature, pressure, etc. [13–16]. To increase the efficiency of the fuel cell, it is very important to have a model to predict the dynamic behavior of the system [1,17–21]. In previous research, like [22], the variation of voltage and current from starting to steady state operation working point is studied. In [23], for example, it is showed that the change of the voltage affects the current; these variations must be taken into account when the fuel cell changes its power.

To avoid these variations in the output, a power system is attached after the fuel cell to establish the voltage to the desired application. Then, the main output signal to control the fuel cell would be the amount of electrical power produced. The model presented in this article predicts the H_2 flow inlet variation, in order to adapt the actual to the desired electrical power at the output of the fuel cell. The model is based on input–output data techniques [22,24–28] that help the control system to be more accurate and efficient [29–35].

A hybrid intelligent model is created by combining clustering and intelligent regression algorithms. These kinds of models were used with good results in several different applications [36–42]. Other algorithms based on multiple regression analysis used to have worse performance, but they are still used [37,43–46]. The hybrid system presented in this paper uses Artificial Neural Networks and Polynomial Regression techniques to perform the regression phase [47–52]. This type of hybrid model allows for obtaining good accuracy in nonlinear systems [53–58].

This paper is organized as follows: after the Introduction, the case study is presented, where the physical system used in the research is presented. The following section is the model approach where the hybrid intelligent model and the algorithms used are described. The results section explains the configuration of the hybrid model and the performance values achieved with the prediction model. Finally, conclusions and future works are depicted.

2. Case Study

Figure 1 shows a PEMFC fuel cell diagram; in this type of cell, the electrolyte is in contact with anodes and cathodes. When there is an inlet flow of hydrogen through the anode and oxygen in the cathode, ions (electrical charges) appear in the electrolyte [59]. In the anode, electrons that flow in an external circuit to the cathode are produced. The ions and the electrons are combined in the cathode to

produce pure water as a residue of the whole reaction. In a normal condition, a single fuel cell can generate 1.2 V. To create high power systems, some single cells can be connected between each other to form a stack; the cell could be in series or parallel.

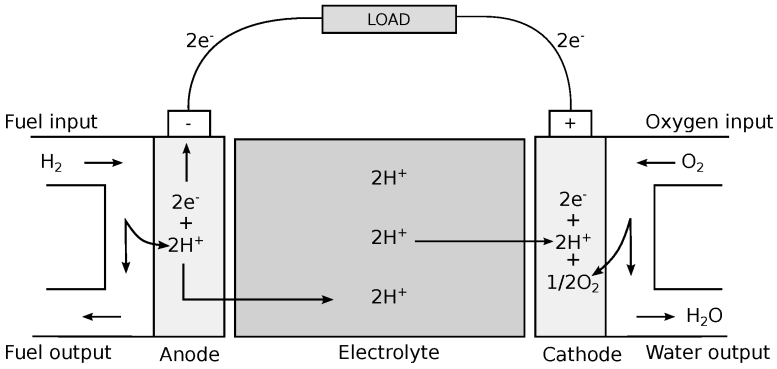

Figure 1. Fuel cell diagram.

2.1. Test Bench

To collect the data for the present research, a test bench in a laboratory has been used. The stack is a PEMFC FCgen-1020AVS from Ballard (Majsmarken, Hobro, Denmark) [60], and it is formed by 80 BAM4G polymeric single cells [61]. The stack has a porous carbon cloth anode and cathode, with catalyst based on platinum [62]. The whole stack has graphite plates between cells, and aluminum end plates, all of them joined by compression.

The maximum output power of the stack is 3.4 kW, with typical values for voltage and current of 45.33 V and 75 A. The stack has its own refrigeration system that cools the stack by air. The pressure of the hydrogen inlet is around 1.36 bar. The stack also has the oxidant subsystem that is built based on the manufacturer's instructions [63]; the cooling system follows these instructions too.

Figure 2 shows the diagram of the Balance of Plant (BoP) system, where all the subsystems are represented. In Figure 3, the real laboratory equipment is shown [64]. To perform different tests, a programmable electronic load was used (Amrel PLA5K-120-1200, San Diego, CA, USA). The monitor system stores all the important values of the stack, as temperature, voltage, current, hydrogen flow, etc., and it is described in [65,66].

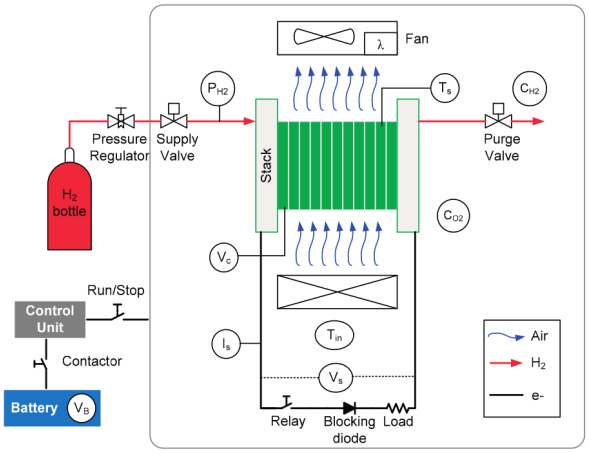

Figure 2. Stack and the Balance of Plant (BoP) to integrate the fuel cell.

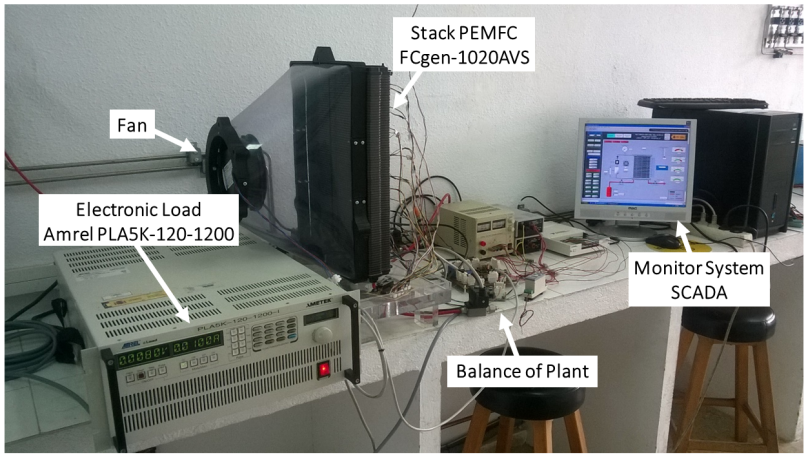

Figure 3. Laboratory implementations to test the fuel cell.

There are several previous works that demonstrate these important values; for example, the authors in [67] studied the effects on the cell operation of stack temperature. In [63], the necessary purge process in the hydrogen that needs to be vented to the atmosphere periodically is studied.

2.2. Power System

As the fuel cell is a system that produces a non-regulated power, it is necessary to include a power system at the output of the cell to adapt the voltage and power values to the ones desired to the specific application, Figure 4.

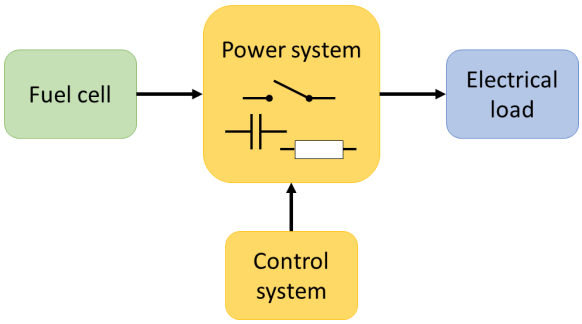

Figure 4. Power system diagram to control cell power output.

The power system should have a stable voltage; the control system would stabilize the variations in the fuel cell produced by the variation of the output power. Then, the main value in the system would be the output power, as the power system controls the voltage and current values.

3. Model Approach

This research is based on the basic model shown in Figure 5a, where the main variables are presented. The model uses the power generated by the fuel cell, the hydrogen inlet flow, and the desired power variation, in order to predict the necessary variation of the hydrogen flow. As it is explained, this research takes into account the amount of power generated by the fuel cell, not the values of current and voltage. With power converters, for example, the voltage variation at the output of the fuel cell can be established at the right value for a specific application.

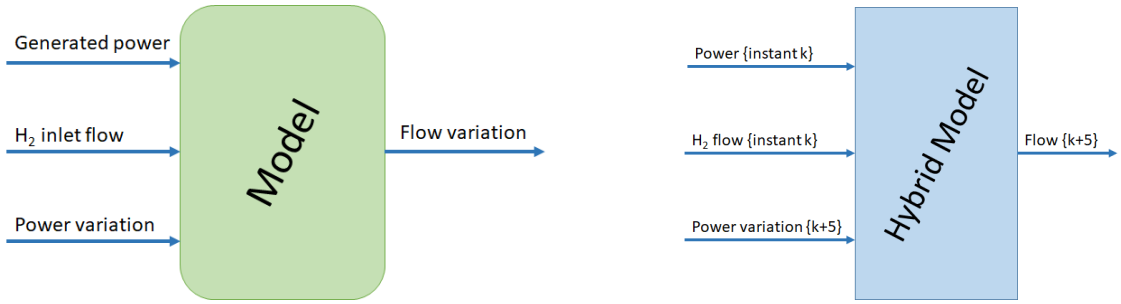

(a) Basic schematic model. **(b)** Model approach

Figure 5. Basic and specific model to predict variation in the hydrogen inlet flow.

Figure 5b shows the timing for specific inputs and output of the model, and also that this research will use a hybrid model. The output of the model is a future prediction; in this case, the model obtains the output with a horizon of five instants in the future. These five instants should be sufficient to adapt the hydrogen inlet control system of the fuel cell to the desired new output power.

The hybrid intelligent system layout is shown in Figure 6; in this figure, it is shown the different local models created for the different clusters. Figure 7 shows the procedure to create the hybrid model.

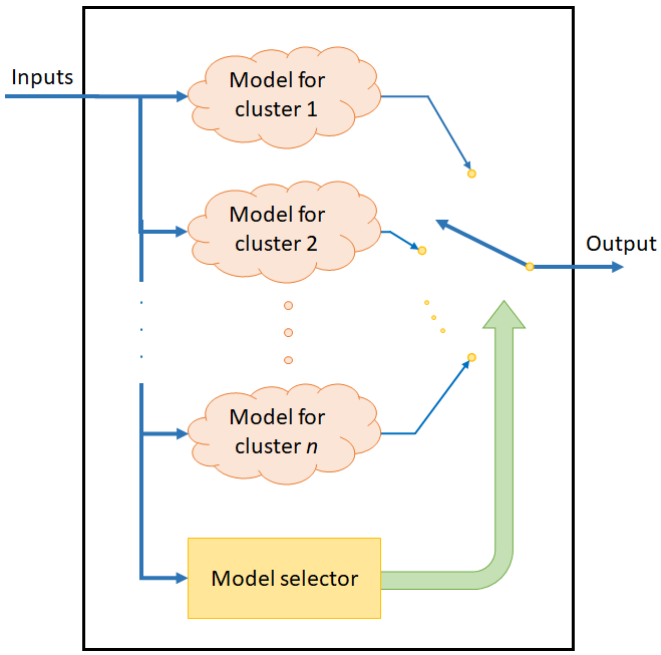

Figure 6. Internal schematic to achieve the hybrid model.

First of all, the clustering phase assigns each training sample to a cluster; the number of clusters used is not known previously, and it is selected in the last phase, after checking the results of all possible hybrid topologies. For each cluster, different configurations of regression techniques were trained. K-Fold cross validation is used to select the best local model that produces the lowest prediction error (Figure 8).

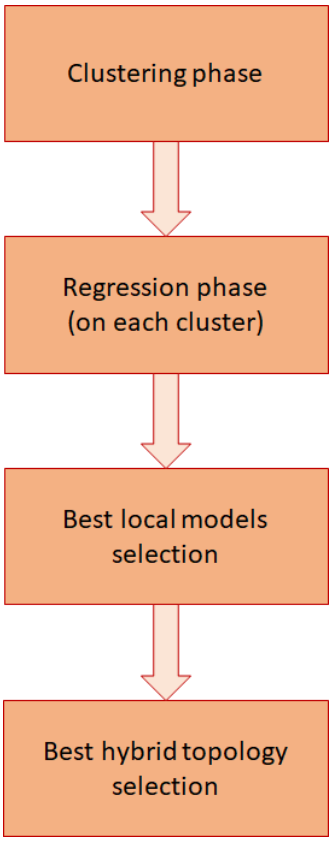

Figure 7. Flowchart of the hybrid model creation phases.

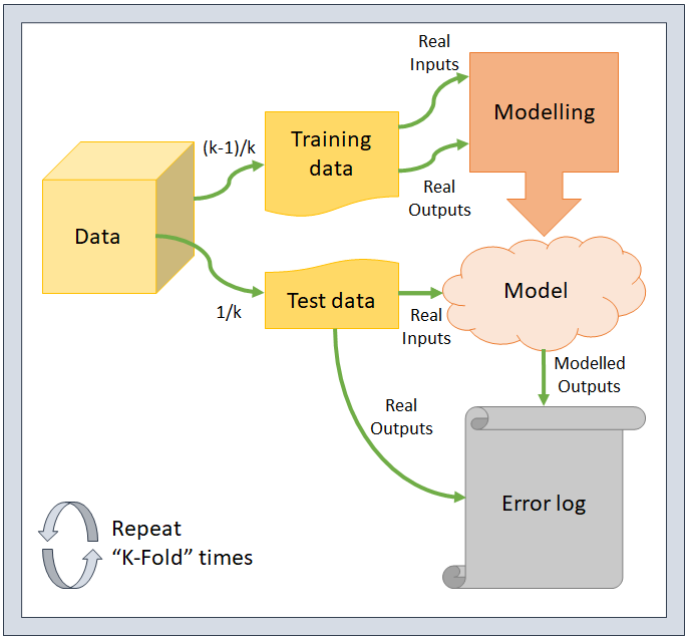

Figure 8. K-Fold training and test data selection.

A more real error measurement is achieved by using K-Fold instead of Hold-Out validation. With K-Fold, all the data are used as testing data, but in different instants; in the case of 10-Fold cross validation, 10 models are created, each one with 90% of the data for training. Each of these 10 models uses the other 10% of the data for testing the model; at the end of the training process, the "Error log" (Figure 8) includes all the available data. Hold-Out validation would divide the data in training and

testing in ratios like 60–40 or 70–30; and only one model would be created. The error was calculated only with this testing data.

The Mean Squared Error is a commonly used error measurement for selecting the best regression local model, in order to choose the best configuration for the regression techniques of each cluster, as the second and third steps in Figure 7 show. After that, it is necessary to select the best hybrid topology, the number of local models to the final hybrid model. To choose this topology, a new testing dataset, isolated at the beginning for the training procedure described below, is used in all the different hybrid models (with different topologies). Each hybrid model produces different errors depending on the internal number of clusters and, with this type of hybrid testing, it is ensured that the best topology is chosen.

3.1. K-Means Algorithm

One of the most known clustering algorithms is the K-Means algorithm. This algorithm creates as many centroids as clusters, and, at the end of the training phase, the centroids are placed in the center of their cluster. The data belonging to each cluster are data with similar characteristics [68,69].

To train the algorithm, in an initial phase, the centroids are randomly chosen from all the data. During the training, these centroids vary their positions to be the center of each cluster. An iterative phase includes the assignment of the cluster for all data samples, taking into account the distances to the centroids. After all, the samples have their "new" cluster, the centroids are calculated another time (as the center of each cluster). The training finishes when the centroids are not moved from the previous iteration [70].

Once the algorithm is trained, a new sample only needs to compare the distance to each centroid to assign a cluster. The usual distance is the Euclidean, and new data are assigned to its cluster very fast [71]. The training phase could finish in local minima; to avoid these situations, it is usual to train several times with random initialization and choose the furthest centroids.

3.2. Artificial Neural Networks

ANN (Artificial Neural Network) is an algorithm used in regression (and in classification) that is based on small units called neurons. The neurons are connected internally with links, and every one calculates its output using an activation function. The input to this activation function is the sum of the input links in the neuron [72].

The ANN algorithm has the ability to generalize through the experience; although the cases are not trained before, the obtained results should be good [73]. This intelligent algorithm creates its own internal representation of a problem, adapting the different links of the neurons [74].

The mentioned activation function used to define the state of a neuron [75]. This state is defined in a normalized range for each ANN—normally [0, 1] or $[-1, 1]$. Depending on the inputs and the selected activation function, the neuron can be inactive (0 or -1) or active (1). In some cases, the neuron could be neither inactive nor active; instead of that, the output would mean an intermediate state between the range.

The internal configuration of the ANN is known as its topology. An ANN could be divided into different layers: input, hidden, and output layer, whose neurons have the same inputs and outputs. The topology defines the links between the neurons and layers, and also the activation functions [76].

The most known architecture of an ANN is the Multi-Layer Perceptron that has a feedforward connections from the input to the output layer (through the hidden layers). Most of the neurons used have a Tan-Sigmoid or Log-Sigmoid activation function; however, the output neurons when the ANN is trained for regression could have a linear function instead.

3.3. Polynomial Regression

The Polynomial regression algorithm is an old technique used to achieve a linear regression function. It is based on some basis functions that are summed [77–81]. The number of inputs and the degree of the used polynomial affect the number of these basis functions.

Different examples of the polynomial are shown in equation (1) and (2)—both of them for two inputs, but with different polynomial degrees:

$$F(x) = a_0 + a_1 x_1 + a_2 x_2, \tag{1}$$

$$F(x) = a_0 + a_1 x_1 + a_2 x_2 + a_3 x_1 x_2 + a_4 x_1^2 + a_5 x_2^2. \tag{2}$$

3.4. Data Processing

The BoP described below collects the data used in this research. All of the data available have 736,339 samples from six different experiments. However, as the model used different time instants for the inputs and outputs, there are some samples that are not used. The number of valid samples to the research was 736,309.

This data were divided in three different sets of data: for training (441,785 samples), to select the hybrid topology (147,262 samples), and, for tests, the final hybrid model (147,262 samples).

4. Results

The results of this research could be divided into four different parts: the clustering, the modelling, the hybrid topology selection, and the test.

4.1. Clustering Results

As it is explained, he K-Means algorithm is used for clustering. With this technique, the training data were divided into nine different hybrid systems, with different numbers of clusters for each one (from 2 to 10). Moreover, the global model (without cluster division) is taken into account.

To ensure good results in the clusters creation, the K-Means algorithm was random initialization of the centroids, and the training was repeated 20 times. These repetitions allow for avoiding finishing the training in a local minima. Table 1 shows the number of samples for each cluster.

Table 1. Number of samples in each created cluster.

	Cl-1	**Cl-2**	**Cl-3**	**Cl-4**	**Cl-5**	**Cl-6**	**Cl-7**	**Cl-8**	**Cl-9**	**Cl-10**
Global	441,785									
Hybrid 2	201,384	240,401								
Hybrid 3	118,308	154,026	169,451							
Hybrid 4	83,452	86,605	117,997	153,731						
Hybrid 5	34,942	83,221	83,286	86,605	153,731					
Hybrid 6	34,942	66,739	83,221	83,286	86,310	87,287				
Hybrid 7	7785	27,157	66,739	83,221	83,286	86,310	87,287			
Hybrid 8	7785	27,157	37,172	51,646	65,208	83,221	83,286	86,310		
Hybrid 9	7785	27,157	30,610	36,146	37,089	50,181	83,221	83,286	86,310	
Hybrid 10	7785	19,961	27,157	30,610	36,146	37,089	50,181	66,478	83,093	83,285

4.2. Modeling Results

To train the regression algorithm (ANN and Polynomial), K-Fold cross validation in the training data was used. As is described, this validation divides the data K times and the final error achieved is a more real measure of the behavior of the system.

The ANNs were configured with only one hidden layer, but the different architectures mean different numbers of neurons in this hidden layer. They have three inputs and one output—tan-sigmoid

as activation function for all the neurons except the output one that has a linear function. The internal neurons varied from 1 to 15.

To train each ANN configuration, the Levenberg–Marquardt optimization algorithm was used. Moreover, to finish the training phase, gradient descent was used as a base on the MSE (mean squared error).

In the case of a polynomial regression algorithm, the configuration varies between the first or second degree, with the same number of inputs and outputs that are described below.

To select the best algorithm and its configuration for each cluster, the MSE as the performance error measurement is used. Table 2 shows the MSE for each cluster, and Table 3 shows the best algorithm for each case.

Table 2. Mean square error for each individual hybrid model ($\cdot 10^{-3}$).

	Cl-1	**Cl-2**	**Cl-3**	**Cl-4**	**Cl-5**	**Cl-6**	**Cl-7**	**Cl-8**	**Cl-9**	**Cl-10**
Global	0.0123									
Hybrid 2	0.0108	0.0149								
Hybrid 3	0.0111	0.0130	0.0091							
Hybrid 4	0.0089	0.0073	0.0114	0.0122						
Hybrid 5	0.0269	0.0120	0.0054	0.0068	0.0124					
Hybrid 6	0.0269	0.0149	0.0121	0.0053	0.0072	0.0095				
Hybrid 7	0.1104	0.0026	0.0138	0.0123	0.0053	0.0069	0.0095			
Hybrid 8	0.1104	0.0027	0.0069	0.0092	0.0140	0.0121	0.0053	0,0071		
Hybrid 9	0.1104	0.0029	0.0199	0.0049	0.0069	0.0092	0.0108	0.0054	0.0069	
Hybrid 10	0.1104	0.0069	0.0027	0.0162	0.0040	0.0068	0.0094	0.0068	0.0122	0.0054

Table 3. Configuration for each individual hybrid model.

	Cl-1	**Cl-2**	**Cl-3**	**Cl-4**	**Cl-5**	**Cl-6**	**Cl-7**	**Cl-8**	**Cl-9**	**Cl-10**
Global	ANN12									
Hybrid 2	ANN14	Poly1								
Hybrid 3	ANN14	ANN12	ANN13							
Hybrid 4	ANN11	ANN11	Poly1	ANN11						
Hybrid 5	Poly1	Poly2	Poly1	ANN12	ANN11					
Hybrid 6	Poly2	ANN13	Poly2	Poly1	ANN14	ANN13				
Hybrid 7	Poly1	ANN11	ANN13	Poly1	Poly1	ANN15	ANN11			
Hybrid 8	Poly1	ANN15	ANN13	ANN14	ANN11	Poly2	Poly1	ANN14		
Hybrid 9	Poly1	ANN13	ANN11	ANN15	ANN15	ANN15	ANN13	Poly1	ANN15	
Hybrid 10	Poly1	ANN15	ANN14	ANN11	ANN15	ANN13	ANN12	ANN14	Poly1	Poly1

4.3. Hybrid Topology Selection

To select the hybrid topology, the number of local models or the global one, a new data set isolated from the training phase described in the previous subsection is used. The models used this new data to calculate the output, and a new error log was achieved for each hybrid topology. Table 4 shows the MSE obtained for each model, where it is possible to choose the configuration with eight clusters, as it has the lowest MSE value.

Table 4. Mean squared error for each model.

Global	**Hybrid Model (Local Models)**								
	2	**3**	**4**	**5**	**6**	**7**	**8**	**9**	**10**
0.1403	0.1405	0.1466	0.2567	0.6253	0.9691	0.3424	0.1204	0.2638	0.2015

According with Table 3, the best hybrid model will have internally different algorithms as Polynomial (first and second degree), and Artificial Neural Networks (with 11, 13, 14, and 15 neurons in the hidden layer). All these models are different—although in the table, the same model configurations

appear, and each model is specific for its cluster. $Poly1^1$ is different than $Poly1^8$ (with superscripts meaning the clusters), in the same way $ANN13^2$ is different than $ANN13^7$, and $ANN15^4$, $ANN15^5$, $ANN15^6$, and $ANN15^9$ are different between each other.

4.4. Test Results

After the hybrid configuration was chosen, the final hybrid model was tested with the final data set isolated from the beginning. Table 5 shows different error measurements for this configuration: MSE, NMSE (Normalized MSE), MAE (Mean Absolute Error), and MAPE (Mean Absolute Percentage Error).

Table 5. Performance values for the best hybrid configuration.

	MSE	NMSE	MAE	MAPE
8 local models configuration	1.2036×10^{-5}	3.1051	5.1196×10^{-4}	819.7600

MSE: Mean Squared Error; NMSE: Normalized Mean Squared Error; MAE: Mean Absolute Error; MAPE: Mean Absolute Percentage Error.

Figure 9 shows the fuel cell inlet flow. The green line was calculated with the actual flow and the simulated variation from the model presented in Table 5, a configuration with eight local models. The blue line is the real hydrogen inlet flow.

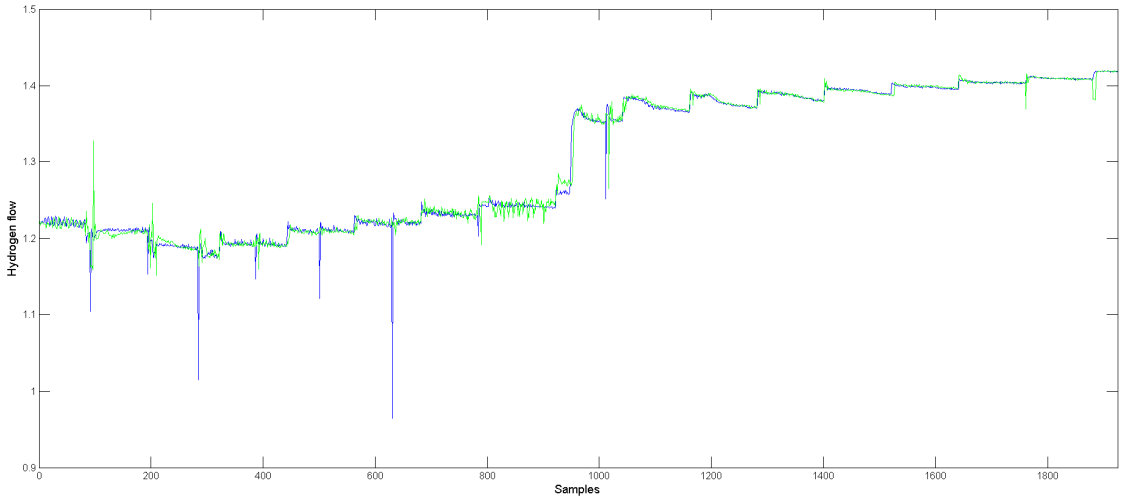

Figure 9. Hydrogen flow calculated with simulated (green) and real (blue) data.

Another simulation using random samples from another test was made. The graphical results (Figure 10) show that the error between the real and simulated data used to be less than 0.1.

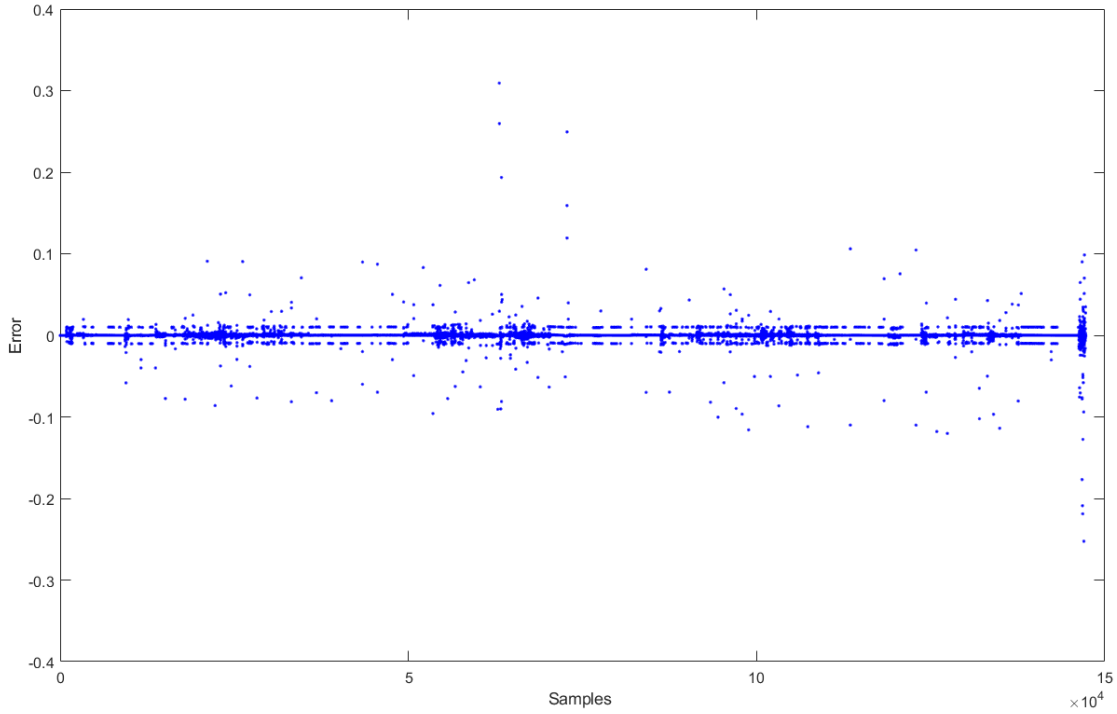

Figure 10. Error between real and simulated values.

5. Conclusions and Future Works

In this research, a new model to predict the variation in the inlet flow rate to change the output power of a fuel cell is developed. The model can predict with very good results this variation, and allow for adapting the hydrogen inlet control system to the desired working point.

As the fuel cell system is nonlinear, a hybrid model is chosen, combining clusters' techniques with ANN and Polynomial regression algorithm. The results show that the best configuration is achieved with eight local models. These models are different topologies of ANN (with 11 to 15 neurons in the hidden layer), and Polynomial regression (first and second degree). The test data used to check the performance of the final model obtained error values like 1.2×10^{-5} for MSE, or 5.1196×10^{-4} for MAE.

As future work, the joining of the prediction variation calculated with the present model, and the control system of the fuel cell, is taken into consideration. It is possible to create an adaptive-predictive control system with the model from this paper; this new control should be faster and better to adapt the fuel cell to the changes desired in the load power.

Author Contributions: Data curation, F.S.M. and A.J.B.; Project administration, J.L.C.-R. and J.M.A.; Software, J.-L.C.-R. and A.J.B.; Validation, F.S.M. and J.M.A.; Writing, original draft, J.-L.C.-R. and J.L.C.-R.

Funding: This work has been funded by the Spanish Ministry of Economy Industry and Competitiveness through the H2SMART-μGRID (DPI2017-85540-R) project.

Conflicts of Interest: The authors declare no conflict of interest.

References

1. Vivas, F.; De las Heras, A.; Segura, F.; Andújar, J. A review of energy management strategies for renewable hybrid energy systems with hydrogen backup. *Renew. Sustain. Energy Rev.* **2018**, *82*, 126–155. [CrossRef]
2. Ghanaatian, M.; Lotfifard, S. Control of Flywheel Energy Storage Systems in the Presence of Uncertainties. *IEEE Trans. Sustain. Energy* **2019**, *10*, 36–45. [CrossRef]
3. Slocum, A.H.; Fennell, G.E.; Dundar, G.; Hodder, B.G.; Meredith, J.D.C.; Sager, M.A. Ocean Renewable Energy Storage (ORES) System: Analysis of an Undersea Energy Storage Concept. *Proc. IEEE* **2013**, *101*, 906–924. [CrossRef]

4. Bruninx, K.; Dvorkin, Y.; Delarue, E.; Pandžić, H.; D'haeseleer, W.; Kirschen, D.S. Coupling Pumped Hydro Energy Storage With Unit Commitment. *IEEE Trans. Sustain. Energy* **2016**, *7*, 786–796. [CrossRef]
5. Andújar, J.M.; Segura, F. Fuel cells: History and updating. A walk along two centuries. *Renew. Sustain. Energy Rev.* **2009**, *13*, 2309–2322. [CrossRef]
6. De las Heras, A.; Vivas, F.; Segura, F.; Andújar, J. From the cell to the stack. A chronological walk through the techniques to manufacture the PEFCs core. *Renew. Sustain. Energy Rev.* **2018**, *96*, 29–45. [CrossRef]
7. Moreira, M.V.; da Silva, G.E. A practical model for evaluating the performance of proton exchange membrane fuel cells. *Renew. Energy* **2009**, *34*, 1734–1741. [CrossRef]
8. Kirubakaran, A.; Jain, S.; Nema, R. A review on fuel cell technologies and power electronic interface. *Renew. Sustain. Energy Rev.* **2009**, *13*, 2430–2440. [CrossRef]
9. Paska, J.; Biczel, P.; Kłos, M. Hybrid power systems—An effective way of utilising primary energy sources. *Renew. Energy* **2009**, *34*, 2414–2421. [CrossRef]
10. Bertoluzzo, M.; Buja, G. Development of Electric Propulsion Systems for Light Electric Vehicles. *Ind. Inf. IEEE Trans.* **2011**, *7*, 428–435. [CrossRef]
11. De las Heras, A.; Vivas, F.; Segura, F.; Redondo, M.; Andújar, J. Air-cooled fuel cells: Keys to design and build the oxidant/cooling system. *Renew. Energy* **2018**, *125*, 1–20. [CrossRef]
12. Ross, D. Power struggle [power supplies for portable equipment]. *IEE Rev.* **2003**, *49*, 34–38. [CrossRef]
13. Andújar, J.M.; Segura, F.; Durán, E.; Rentería, L.A. Optimal interface based on power electronics in distributed generation systems for fuel cells. *Renew. Energy* **2011**, *36*, 2759–2770. [CrossRef]
14. Segura, F.; Andújar, J.M.; Durán, E. Analog Current Control Techniques for Power Control in PEM Fuel-Cell Hybrid Systems: A Critical Review and a Practical Application. *IEEE J. IE* **2011**, *58*, 1171–1184. [CrossRef]
15. Lekube, J.; Garrido, A.J.; Garrido, I.; Otaola, E. Output Power Improvement in Oscillating Water Column-based Wave Power Plants. *Rev. Iberoam. Autom. Inf. Ind.* **2018**, *15*, 145–155. [CrossRef]
16. Jove, E.; Casteleiro-Roca, J.L.; Quintiá, H.; Méndez-Pérez, J.A.; Calvo-Rolle, J.L. Anomaly detection based on intelligent techniques over a bicomponent production plant used on wind generator blades manufacturing. *Rev. Iberoam. Autom. Inf. Ind.* **2019**, [CrossRef]
17. Amphlett, J.C.; Baumert, R.M.; Mann, R.F.; Peppley, B.A.; Roberge, P.R.; Harris, T.J. Performance modeling of the Ballard Mark IV solid polymer electrolyte fuel cell I. Mechanistic model development. *J. Electrochem. Soc.* **1995**, *142*, 1–8. [CrossRef]
18. Amphlett, J.C.; Mann, R.F.; Peppley, B.A.; Roberge, P.R.; Rodrigues, A. A model predicting transient responses of proton exchange membrane fuel cells. *J. Power Sources* **1996**, *61*, 183–188. [CrossRef]
19. Famouri, P.; Gemmen, R. Electrochemical circuit model of a PEM fuel cell. In Proceedings of the Power Engineering Society General Meeting, Toronto, ON, Canada, 13–17 July 2003; Volume 3, pp. 1436–1440. [CrossRef]
20. Kim, J.; Lee, S.M.; Srinivasan, S.; Chamberlin, C.E. Modeling of proton exchange membrane fuel cell performance with an empirical equation. *J. Electrochem. Soc.* **1995**, *142*, 2670–2674. [CrossRef]
21. Van Bussel, H.; Koene, F.; Mallant, R.K. Dynamic model of solid polymer fuel cell water management. *J. Power Sources* **1998**, *71*, 218–222. [CrossRef]
22. Barragán, A.J.; Al-Hadithi, B.M.; Jiménez, A.; Andújar, J.M. A general methodology for online TS fuzzy modeling by the extended Kalman filter. *Appl. Soft Comput.* **2014**, *18*, 277–289. [CrossRef]
23. Ziogou, C.; Voutetakis, S.; Papadopoulou, S.; Georgiadis, M. Modeling, simulation and experimental validation of a PEM fuel cell system. *Comput. Chem. Eng.* **2011**, *35*, 1886–1900. [CrossRef]
24. López-Baldán, M.J.; García-Cerezo, A.; Cejudo, J.M.; Romero, A. Fuzzy modeling of a thermal solar plant. *Int. J. Intell. Syst.* **2002**, *17*, 369–379. [CrossRef]
25. Ogaji, S.; Singh, R.; Pilidis, P.; Diacakis, M. Modelling fuel cell performance using artificial intelligence. *J. Power Sources* **2006**, *154*, 192–197. [CrossRef]
26. Wojciechowski, S. A comparison of classification strategies in rule-based classifiers. *Log. J. IGPL* **2018**, *26*, 29–46. [CrossRef]
27. Segovia, F.; Górriz, J.M.; Ramírez, J.; Martinez-Murcia, F.J.; García-Pérez, M. Using deep neural networks along with dimensionality reduction techniques to assist the diagnosis of neurodegenerative disorders. *Log. J. IGPL* **2018**, *26*, 618–628. [CrossRef] [PubMed]
28. Andújar, J.M.; Bravo, J.; Peregrín, A. Stability analysis and synthesis of multivariable fuzzy systems using interval arithmetic. *Fuzzy Sets Syst.* **2004**, *148*, 337–353. [CrossRef]

29. Barragán, A.J.; Al-Hadithi, B.M.; Andújar, J.M.; Jiménez, A. Formal methodology for analyzing the dynamic behavior of nonlinear systems using fuzzy logic. *Rev. Iberoam. Autom. Inf. Ind.* **2015**, *12*, 434–445. [CrossRef]
30. Gordillo, F.; Aracil, J.; Alamo, T. Determining limit cycles in fuzzy control systems. *IEEE Int. Conf. Fuzzy Syst.* **1997**, *1*, 193–198. [CrossRef]
31. González, G.; Angelo, C.D.; Forchetti, D.; Aligia, D. Detection and Isolation of Faults on the Rotor Side Converter of Doubly Fed Induction Generators. *Rev. Iberoam. Autom. Inf. Ind.* **2018**, *15*, 297–308. [CrossRef]
32. Fontanet, J.G.G.; Cervantes, A.L.; Ortiz, I.B. Alternatives of Control for a Furuta's Pendulum. *Rev. Iberoam. Autom. Inf. Ind.* **2016**, *13*, 410–420. [CrossRef]
33. Irigoyen, E.; Miñano, G. A NARX neural network model for enhancing cardiovascular rehabilitation therapies. *Neurocomputing* **2013**, *109*, 9–15. [CrossRef]
34. Márquez, J.M.A.; Piña, A.J.B.; Arias, M.E.G. A general and formal methodology for designing stable nonlinear fuzzy control systems. *IEEE J. FUZZ* **2009**, *17*, 1081–1091. [CrossRef]
35. Javier Barragán, A.; Enrique, J.M.; Calderón, A.J.; Andújar, J.M. Discovering the dynamic behavior of unknown systems using fuzzy logic. *Fuzzy Optim. Decis. Mak.* **2018**, *17*, 421–445. [CrossRef]
36. Subia, V.H.; Cedillo, B.L.; Ferragud, F.B.; Durá, J.H. Multi-objective Optimization in Modeling and Control for Rotary Inverted Pendulum. *Rev. Iberoam. Autom. Inf. Ind.* **2018**, *15*, 363–373. [CrossRef]
37. Calvo-Rolle, J.L.; Quintian-Pardo, H.; Corchado, E.; del Carmen Meizoso-López, M.; García, R.F. Simplified method based on an intelligent model to obtain the extinction angle of the current for a single-phase half wave controlled rectifier with resistive and inductive load. *J. Appl. Log.* **2015**, *13*, 37–47. [CrossRef]
38. Calvo-Rolle, J.L.; Fontenla-Romero, O.; Pérez-Sánchez, B.; Guijarro-Berdinas, B. Adaptive Inverse Control Using an Online Learning Algorithm for Neural Networks. *Informatica* **2014**, *25*, 401–414. [CrossRef]
39. Jove, E.; Gonzalez-Cava, J.M.; Casteleiro-Roca, J.L.; Méndez-Pérez, J.A.; Antonio Reboso-Morales, J.; Javier Pérez-Castelo, F.; Javier de Cos Juez, F.; Luis Calvo-Rolle, J. Modelling the hypnotic patient response in general anaesthesia using intelligent models. *Log. J. IGPL* **2018**, *27*, 189–201. [CrossRef]
40. Jove, E.; Antonio Lopez-Vazquez, J.; Isabel Fernandez-Ibanez, M.; Casteleiro-Roca, J.L.; Luis Calvo-Rolle, J. Hybrid Intelligent System to Predict the Individual Academic Performance of Engineering Students. *Int. J. Eng. Educ.* **2018**, *34*, 895–904.
41. Jove, E.; Blanco-Rodríguez, P.; Casteleiro-Roca, J.L.; Moreno-Arboleda, J.; López-Vázquez, J.A.; de Cos Juez, F.J.; Calvo-Rolle, J.L. Attempts prediction by missing data imputation in engineering degree. In Proceedings of the International Joint Conference SOCO'17-CISIS'17-ICEUTE'17 León, Spain, 6–8 September 2017; pp. 167–176.
42. Andújar, J.M.; Bravo, J.M. Multivariable fuzzy control applied to the physical-chemical treatment facility of a Cellulose factory. *Fuzzy Sets Syst.* **2005**, *150*, 475–492. [CrossRef]
43. Zapata, F.E.; Galilea, J.L.; Bueno, J.O. ALCOR Project: Contributions to Optimizing Remote Robot Guidance in Intelligent Spaces. *Rev. Iberoam. Autom. Inf. Ind.* **2018**, *15*, 416–426. [CrossRef]
44. Chalki, A.; Koutras, C.D.; Zikos, Y. A quick guided tour to the modal logic S4.2. *Log. J. IGPL* **2018**, *26*, 429–451. [CrossRef]
45. Rincon, J.A.; Julian, V.; Carrascosa, C.; Costa, A.; Novais, P. Detecting emotions through non-invasive wearables. *Log. J. IGPL* **2018**, *26*, 605–617. [CrossRef]
46. Tomás-Rodríguez, M.; Santos, M. Modelling and control of floating offshore wind turbines. *Rev. Iberoam. Autom. Inf. Ind.* **2019**, *16*, 381–390. [CrossRef]
47. García, R.F.; Rolle, J.L.C.; Gomez, M.R.; Catoira, A.D. Expert condition monitoring on hydrostatic self-levitating bearings. *Expert Syst. Appl.* **2013**, *40*, 2975–2984. [CrossRef]
48. Molina-Cabello, M.A.; López-Rubio, E.; M Luque-Baena, R.; Domínguez, E.; Palomo, E.J. Foreground object detection for video surveillance by fuzzy logic based estimation of pixel illumination states. *Log. J. IGPL* **2018**, *26*, 593–604. [CrossRef]
49. García, R.F.; Rolle, J.L.C.; Castelo, J.P.; Gomez, M.R. On the monitoring task of solar thermal fluid transfer systems using NN based models and rule based techniques. *Eng. Appl. Artif. Intell.* **2014**, *27*, 129–136. [CrossRef]
50. Quintián, H.; Calvo-Rolle, J.L.; Corchado, E. A Hybrid Regression System Based on Local Models for Solar Energy Prediction. *Informatica* **2014**, *25*, 265–282. [CrossRef]
51. Quintian Pardo, H.; Calvo Rolle, J.L.; Fontenla Romero, O. Application of a low cost commercial robot in tasks of tracking of objects. *Dyna* **2012**, *79*, 24–33.

52. Moreno-Fernandez-de Leceta, A.; Lopez-Guede, J.M.; Ezquerro Insagurbe, L.; Ruiz de Arbulo, N.; Graña, M. A novel methodology for clinical semantic annotations assessment. *Log. J. IGPL* **2018**, *26*, 569–580. [CrossRef]
53. Alaiz Moretón, H.; Calvo Rolle, J.; García, I.; Alonso Alvarez, A. Formalization and practical implementation of a conceptual model for PID controller tuning. *Asian J. Control* **2011**, *13*, 773–784. [CrossRef]
54. Rolle, J.; Gonzalez, I.; Garcia, H. Neuro-robust controller for nonlinear systems. *Dyna* **2011**, *86*, 308–317. [CrossRef]
55. Gonzalez-Cava, J.M.; Reboso, J.A.; Casteleiro-Roca, J.L.; Calvo-Rolle, J.L.; Méndez Pérez, J.A. A novel fuzzy algorithm to introduce new variables in the drug supply decision-making process in medicine. *Complexity* **2018**, *2018*. [CrossRef]
56. Burduk, A.; Bozejko, W.; Pempera, J.; Musial, K. On the simulated annealing adaptation for tasks transportation optimization. *Log. J. IGPL* **2018**, *26*, 581–592. [CrossRef]
57. Casteleiro-Roca, J.L.; Barragán, A.J.; Segura, F.; Calvo-Rolle, J.L.; Andújar, J.M. Intelligent hybrid system for the prediction of the voltage-current characteristic curve of a hydrogen-based fuel cell. *Rev. Iberoam. Autom. Inf. Ind.* **2019**, *16*, 492–501. [CrossRef]
58. de la Portilla, M.P.; Piñeiro, A.L.; Sánchez, J.A.S.; Herrera, R.M. Dynamic Modelling and Control of a Submerged Device with Hydrostatic Actuators. *Rev. Iberoam. Autom. Inf. Ind.* **2017**, *15*, 12–23. [CrossRef]
59. Andújar, J.M.; Segura, F.; Vasallo, M.J. A suitable model plant for control of the set fuel cell–DC/DC converter. *Renew. Energy* **2008**, *33*, 813–826. [CrossRef]
60. Ballard. FCgen1020-ACS fuel cell from Ballard Power Systems. Available online: http://www.ballard.com/docs/default-source/backup-power-documents/fcgen-1020acs.pdf (accessed on 15 October 2018).
61. Mehta, V.; Cooper, J. Review and analysis of PEM fuel cell design and manufacturing. *J. Power Sources* **2003**, *114*, 32–53. [CrossRef]
62. Ralph, T.; Hards, G.; Keating, J.; Campbell, S.; Wilkinson, D.; Davis, M.; St-Pierre, J.; Johnson, M. Low cost electrodes for proton exchange membrane fuel cells: Performance in single cells and Ballard stacks. *J. Electrochem. Soc.* **1997**, *144*, 3845–3857. [CrossRef]
63. Ballard. FCgenTM-1020ACS/FCvelocityTM-1020ACS Fuel Cell Stack. Ballard Product Manual and Integration Guide. Document Number MAN5100192-0GS. Available online: https://www.ballard.com/fuel-cell-solutions/fuel-cell-power-products/fuel-cell-stacks (accessed on 9 November 2019)
64. Segura, F.; Andújar, J. Step by step development of a real fuel cell system. Design, implementation, control and monitoring. *Int. J. Hydrog. Energy* **2015**, *40*, 5496–5508. [CrossRef]
65. Segura, F.; Andújar, J. Modular PEM fuel cell SCADA & simulator system. *Resources* **2015**, *4*, 692–712. [CrossRef]
66. Segura, F.; Bartolucci, V.; Andújar, J. Hardware/software data acquisition system for real time cell temperature monitoring in air-cooled polymer electrolyte fuel cells. *Sensors (Switzerland)* **2017**, *17*. [CrossRef] [PubMed]
67. Li, X.; Deng, Z.H.; Wei, D.; Xu, C.S.; Cao, G.Y. Parameter optimization of thermal-model-oriented control law for PEM fuel cell stack via novel genetic algorithm. *Energy Convers. Manag.* **2011**, *52*, 3290–3300. [CrossRef]
68. MacQueen, J. Some methods for classification and analysis of multivariate observations. In Proceedings of the Fifth Berkeley Symposium on Mathematical Statistics and Probability, Oakland, CA, USA, June 21–July 18, 1965 and December 27, 1965-January 7, 1966; Volume 1, pp. 281–297.
69. Moody, J.; Darken, C. Fast Learning in Networks of Locally-Tuned Processing Units. *Neural Comput.* **1989**, *1*, 281–294. [CrossRef]
70. Viñuela, P.; León, I. *Redes de Neuronas Artificiales: Un Enfoque Práctico*; Pearson Educación: Prentice Hall, NJ, USA, 2004.
71. Orallo, J.; Quintana, M.; Ramírez, C. *Introducción a la Minería de Datos*; Editorial Alhambra S.A.: Madrid, Spain, 2004.
72. Galipienso, M.; Quevedo, M.; Pardo, O.; Ruiz, F.; Ortega, M. *Inteligencia artificial. Modelos, técnicas y áreas de aplicación*; Editorial Paraninfo: Madrid, Spain, 2003.
73. González, J.; Hernando, V. *Redes Neuronales Artificiales: Fundamentos, Modelos y Aplicaciones*; Ra-Ma: Madrid, Spain, 2000.
74. Harston, A.M.C.; Pap, R. *Handbook of Neural Computing Applications*; Elsevier Science: Amsterdam, The Netherlands, 2014.

75. del Brío, B.; Molina, A. *Redes Neuronales y Sistemas Borrosos*; Ra-Ma: Madrid, Spain, 2006.
76. López, R.; Fernández, J. *Las Redes Neuronales Artificiales*; Netbiblo S.L.: Oleiros, Spain, 2008.
77. Bishop, C. *Pattern Recognition and Machine Learning (Information Science and Statistics)*; Springer-Verlag New York, Inc.: Secaucus, NJ, USA, 2006.
78. Casteleiro-Roca, J.L.; Barragán, A.J.; Segura, F.; Calvo-Rolle, J.L.; Andújar, J.M. Fuel cell output current prediction with a hybrid intelligent system. *Complexity* **2019**, *2019*. [CrossRef]
79. Heiberger, R.; Neuwirth, E. Polynomial regression. In *R Through Excel*; Springer: New York, NY, USA, 2009; pp. 269–284. [CrossRef]
80. Wu, X. *Optimal Designs for Segmented Polynomial Regression Models and Web-Based Implementation of Optimal Design Software*; State University of New York at Stony Brook: Stony Brook, NY, USA, 2007.
81. Zhang, Z.; Chan, S. On kernel selection of multivariate local polynomial modelling and its application to image smoothing and reconstruction. *J. Signal Process. Syst.* **2011**, *64*, 361–374. [CrossRef]